JOURNAL OF MATERIALS SCIENCE 16 (1981) 1557–1566

Effect of high temperature thermomechanical treatment on the mechanical properties of vanadium-modified AISI 4330 steel

JAI SUNG LEE, JOHN S. CHUN
Korea Advanced Institute of Science, Department of Materials Science, Seoul, Korea

The relationships between the recovery and recrystallization of hot-deformed austenite grains and the precipitation of carbide on tempering in a 0.3C–Ni–Cr–Mo–V steel have been studied to examine closely the favourable effects of high-temperature thermomechanical treatment (HTMT) on the mechanical properties in steel. The results show that the strength and toughness increase with increasing degree of deformation by HTMT, particularly in which the ductile–brittle transition temperature as a measure of toughness decreases steeply with increasing degree of deformation. From the analysis of line broadening on $(1\,1\,0)_M$ and hardness change with holding time after hot deformation, the dynamic recovery and recrystallization during HTMT are believed not to occur. Owing to this, the random distribution of fine carbide precipitates in martensite structure is hardly affected. Consequently, the improvement of mechanical properties by HTMT is due to the distribution of fine carbide precipitates within martensite lath and the refinement of the martensite structure.

1. Introduction

Although high-temperature thermomechanical treatment (HTMT) is recognized as a highly effective form of non-conventional heat treatment for improvement of mechanical properties of steel [1–3], further research is needed to advance the knowledge of the mechanisms of this process. Most studies [4–10] have concentrated on comparisons between HTMT and conventional treatment (CT), to prove its advantages. These studies have been concerned with fracture toughness, crack propagation resistance and behaviour under various environmental conditions. Many studies have been made on structural-grade steels, Fe–Ni–C alloys and Mn–Si–Cr–Mo steel [6, 11]. It is generally believed that HTMT improvement is due mainly to the refinement of austenite grain and martensite structure.

Recently [11], it has been suggested that HTMT improvement can be attributed not only to grain refinement but also to the limitation of dynamic effects of martensite platelets during phase transformation.

It might be expected that some of the favourable effects of HTMT are partially offset due to the recovery and recrystallization of austentite grains during hot deformation. Bol'shakov *et al.* [12] reported that a low alloy steel containing nickel, chromium and molybdenum tended to delay the adverse effects of recovery and recrystallization and so the HTMT process is little influenced.

Vankataraman and Mallik [13, 14] suggested that since the dislocation density would be lower due to the recovery during hot deformation, little carbide precipitation would result, so that incremental strengthening by HTMT was mainly due to the reduction in martensite lath size. Their experimental results were not conclusive and tended to differ from those of previous studies [11].

It is apparent that research is needed to investigate the complex mechanisms involved in the HTMT process.

Vanadium-modified AISI 4330 steel was chosen for HTMT study since it is a widely-used steel. The object of this study was to examine the effects of the precipitation of carbide during tempering

0022–2461/81/061557–10$03.00/0

TABLE I Chemical composition of the specimen (wt%)

C	Si	Mn	Ni	Cr	Mo	V	P	S
0.32	0.28	0.61	2.24	0.93	0.56	0.11	0.008	0.012

and recovery and recrystallization during hot deformation on the mechanical properties of this steel.

2. Experiemntal procedure

2.1. Specimens

The chemical analysis of vanadium-modified AISI 4330 steel used in the experiments is shown in Table I. The melt was prepared in an electric induction furnace and 100 kg ingots were homogenized at 1250° C for 15 h, then hot-forged into 80 mm diameter bars and annealed. These billets were machined to 65 mm diameter, then hot-forged into rectangular sections 60 mm × 50 mm for impact testing and 100 mm × 20 mm for tensile testing. The impact specimens were cut into discs 13.0 to 32.5 mm thick depending the amount of HTMT deformation (0% to 60%) to obtain a final thickness after treatment of 13.0 mm. The tensile specimens were cut 6 to 15 mm thick for a final HTMT thickness of 6.0 mm.

2.2. High temperature thermomechanical treatment (HTMT)

The specimens were solution heat-treated for 1 h at 1000° C to ensure complete dissolution of carbides in the austenite structure. They were immediately transferred into a 900° C constant temperature furnace until forged. A 453 kg hammer, pneumatic forge was used to deform specimens at a rate of 115 strokes per minute. The final dimension was controlled by a hardened steel stop on the anvil. This forging process took from 1 to 5 sec (2 to 8 strokes). The final temperature before water quenching varied between 885 and 897° C since the specimen cooling rate was about 3° C sec^{-1}. One set of specimens was forged at 60% deformation (HTMT 60%) and held at 900° C from 1 to 20 min before water quenching to study austenite grain recovery and recrystallization.

Fig. 1 illustrates the HTMT process. The AC_1 and AC_3 temperatures were measured by a dilatometer. After quenching, another set of specimens was tempered at 600° C from 1 to 100 h and hardness tested. All other specimens were tempered at 600° C for 1 h.

2.3. Testing

Tensile specimens machined to dimensions shown in Fig. 2 were tested on an Instron testing machine at a constant strain rate of 6.67×10^{-4} sec^{-1} at room temperature. Yield strength was determined as the stress level at the 0.2% strain off-set point.

Rockwell C hardness was measured on specimens of various tempering times which were cut and polished to eliminate any decarburized layer.

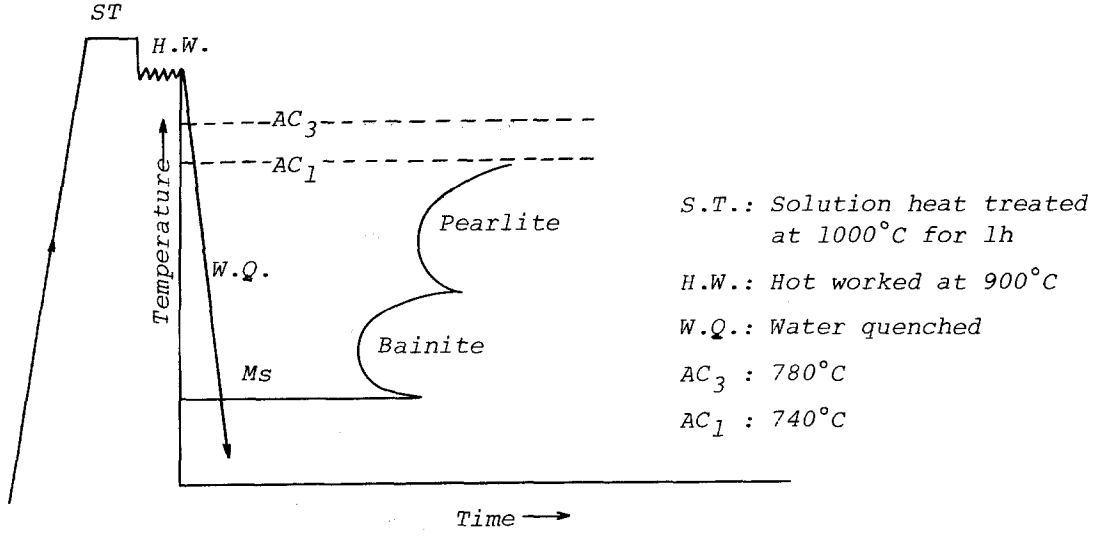

Figure 1 Schematic diagram of high-temperature thermomechanical treatment.

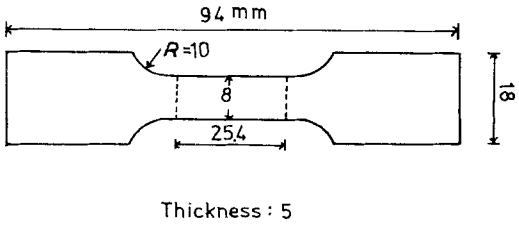

Figure 2 Schematic diagram of tensile specimen.

Toughness was measured on a V-notched charpy tester performed in accordance with ASTM specification E23-72. Test temperatures were varied between − 196 and 100° C. For the various degrees of deformation, the ductile–brittle transition temperature was determined.

2.4. Microscopic observation

Metallographic observation was carried out on prior austenite grain and martensite struture. The austenite grain boundary was revealed by chemical etching in 100 ml saturated aqueous solution of picric acid containg 80 mg cupric chloride and 60 ml wetting agent (Agepon), and the martensite structure was etched in nitrl solution. X-ray diffraction analysis was conducted on $(1\,1\,0)_M$ profiles since this diffraction plane in martensite structure gives the largest intensity. The breadth of this X-ray diffraction profile was used to ascertain the development of recovery and recrystallization during HTMT based on the Tushinskii technique [15]. Precipitation and distribution of carbide precipitates were examined by the carbon extraction replica method under a Hitachi JEM-30 transmission electron microscope operated at 125 kV. The fracture surface on the impact-tested specimen was examined under a JEOL JSM-35 scanning electron microscope.

3. Experimental results and discussion

3.1. Microstructures and carbide precipitation

Fig. 3a and b show the typical microstructures of the CT (conventional heat-treated) and HTMT 54% specimens for the quenched condition. Both quenched specimens reveal martensite structure. An interesting observation is that the HTMT specimen has finer martensite laths in comparison to the CT specimen. The formation of fine martensite structure in the HTMT specimen can be attributed to the higher dislocation density in the course of deformation resulting in the formation of cell structure.

Fig. 4a and b show the morphology and distribution of precipitates in the CT and HTMT 54% specimens after tempering at 600° C for 1 h from the observation of carbon extraction replica. The CT specimen reveals a large number of rod-like coarse cementite precipitates near the martensite lath boundary, while the HTMT specimen shows the distribution of a fine carbide precipitate mainly within martensite laths. In this case, the precipitates were identified by the electron diffraction ring pattern shown in Fig. 5a and b. From the analysis of diffraction patterns, it was found that the precipitates consisted of several types of carbide such as Fe_3C, $(Cr, Fe)_7C_3$, $VC_{0.88}$, and

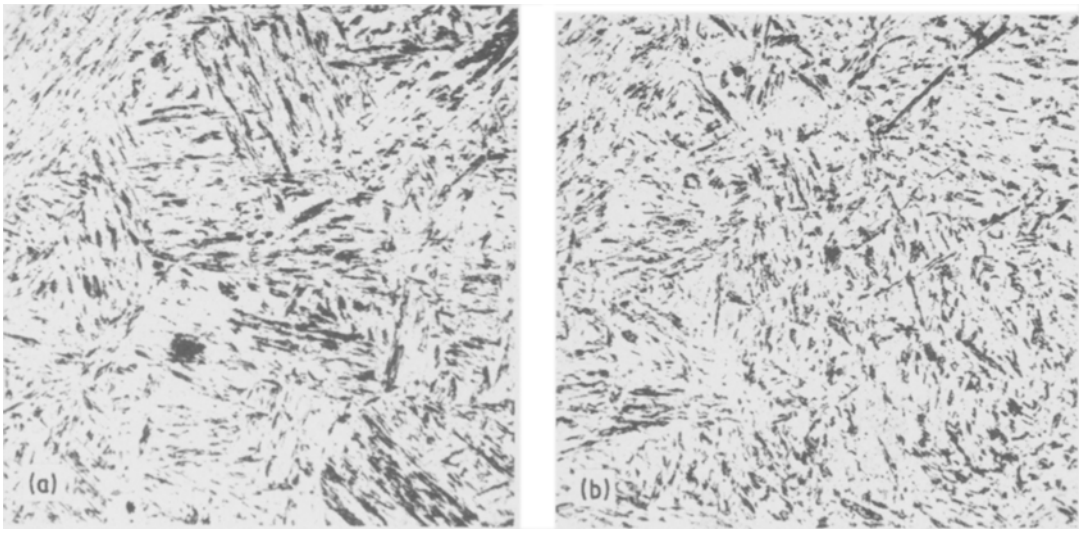

Figure 3 Micrographs of martensite structures of as-quenched specimens (× 420). (a) CT, (b) HTMT 54%.

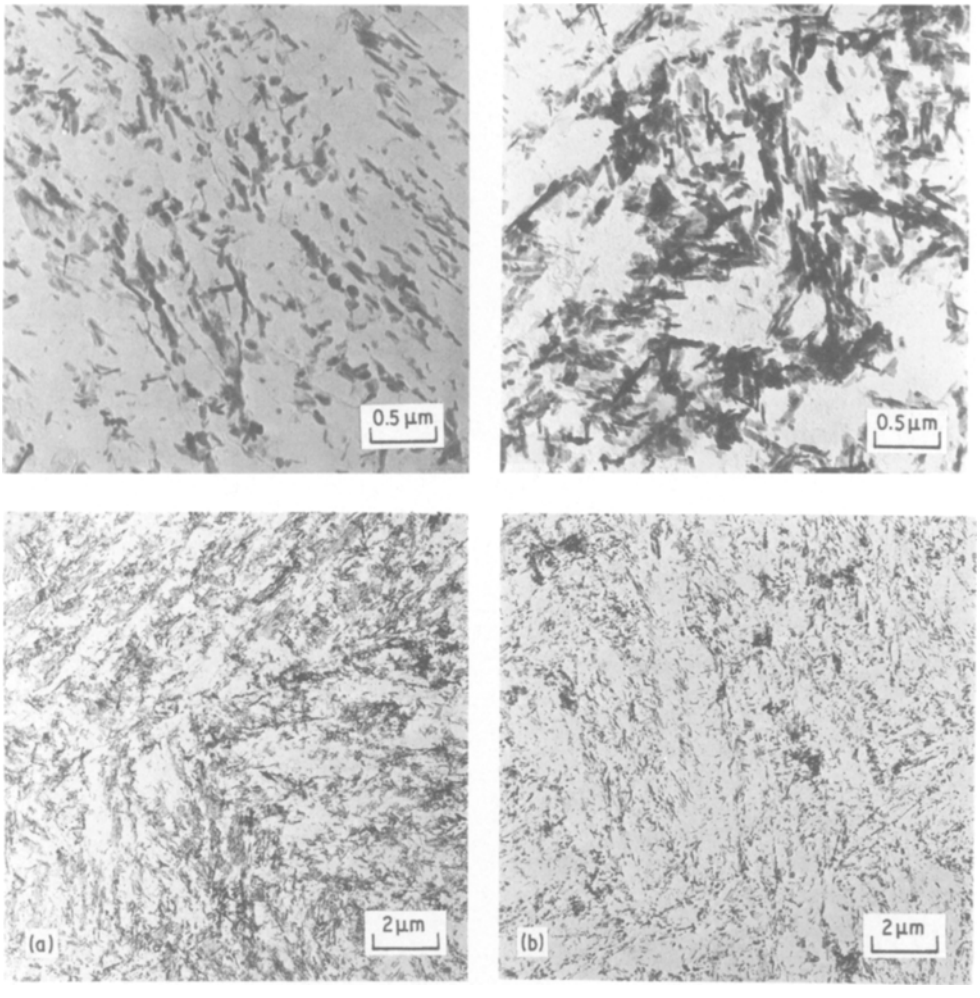

Figure 4 Microstructures of precipitated carbides from carbon extraction replicas (tempered at 600° C for 1 h). (a) CT, (b) HTMT 54%.

Mo_2C. Furthermore, in the case of the HTMT specimen (Fig. 5b) a stronger ring pattern was observed, compared to the CT specimen (Fig. 5a) which means that fine alloy carbides were predominately precipitated by HTMT. These results on the effect of HTMT on precipitation of carbide agree well with other studies [7–9]. On the basis of the tempering mechanism in steel [16, 17], the effect of HTMT on the precipitation of carbide during tempering can be explained as follows. As is well known, the dislocation density is higher in the course of deformation so that within the martensite structure after HTMT, a higher dislocation density will also remain. Moreover, since the dislocation acts as a more energetically favourable site for carbon segregation than normal interstitial sites during autotempering or in the primary stage of tempering, it follows that the tendency for carbon segregation will be higher in the HTMT specimen. If this tendency increases, the carbide cannot help being finely precipitated due to the lack of carbon atoms for formation of carbide which is followed by a slow growth of carbide. In this respect, it can be concluded that HTMT promotes the distribution of fine carbide precipitates randomly in the martensite structure.

3.2. Acceleration of carbide precipitation

Fig. 6 shows the change of hardness with tempering time at 600° C. It was found that tempering resistance corresponding to secondary hardening occurs more rapidly as the degree of deformation increases. This phenomenon indicates that HTMT accelerates the process of carbide precipitation in which the fine alloy carbide leading to tempering resistance (secondary hardening) is gradually

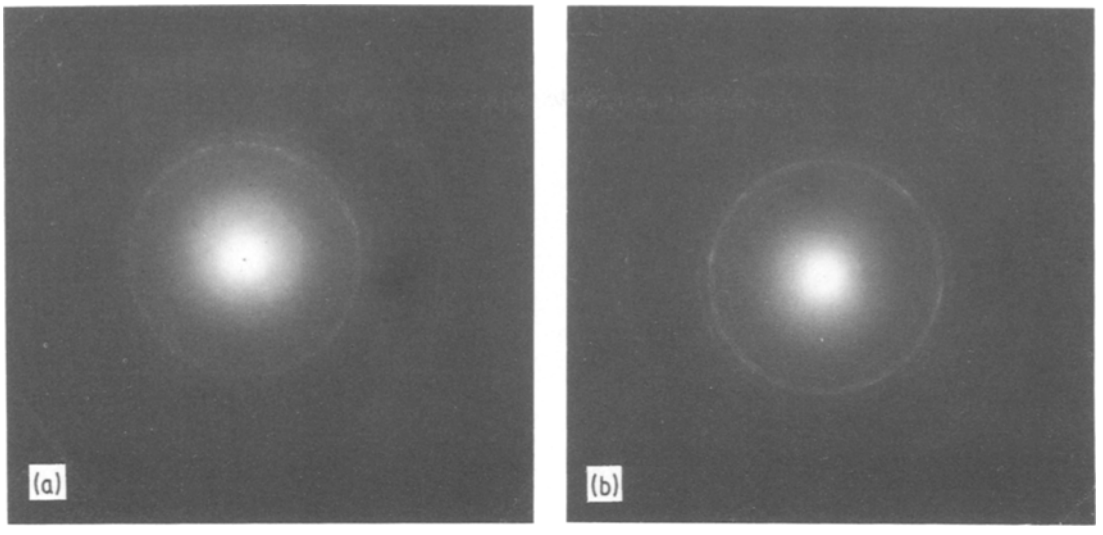

Figure 5 Electron diffraction patterns of precipitated carbides. (a) CT, (b) HTMT 54%.

substituted for the course cementite carbide during tempering at 600° C [18]. Additionally, it was seen in Fig. 5b that the precipitates in the HTMT specimen were identified mainly as fine alloy carbides [$(Cr, Fe)_7C_3$, $VC_{0.88}$, Mo_2C] causing secondary hardening. Furthermore, the acceleration of carbide precipitation is thought to result from the increased vacancy concentration and the local residual strain caused by HTMT which create more opportunities for the nucleation of carbide and greater mobility of carbide-forming elements [18]. In addition to this, it was found that the integral line breadth increases linearly with an increasing degree of deformation (Fig. 7). From the fact [19] that line broadening is due to the existence of crystal defects, grain refinement, etc., this increase of line breadth in Fig. 7 means that HTMT increases the vacancy concentration and dislocation density resulting in local strain. For this reason, it can be concluded that the kinetics of carbide precipitation during tempering is enhanced by the HTMT process.

3.3. Recovery and recrystallization during hot deformation

In this respect, for the purpose of confirming the occurrence of dynamic recovery and recrystallization in the HTMT process on the basis of the

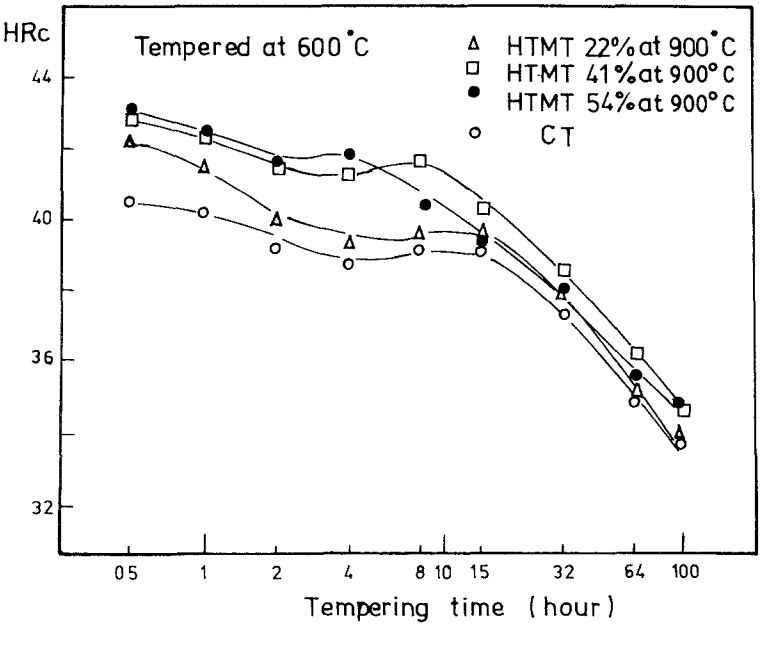

Figure 6 Effect of HTMT on hardness as a function of tempering time.

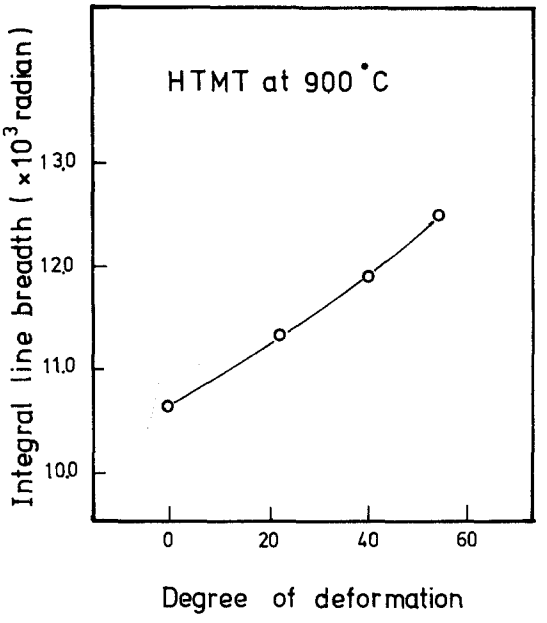

Figure 7 Effect of degree of deformation on $(1\,1\,0)_M$ integral line-breadth.

work of Tushinskii *et al.* [15], both specimen hardness and Tushinskii line-breadth [15] were measured for holding times at 900° C from 1 to 20 min after deformation. The results are shown in Fig. 8, in which the curves coincide well with those of Tushinskii. In the first section of the curves (up to 1 min), the hardness of specimen remains unchanged and the line breadth also changes little during this period, which may be related to the occurrence of static recovery. The existence of this period means that during the hot deformation of austenite, recrystallization does not occur, since deformation ends at the primary stage of dynamic recovery. The second section of the curves (from 1 to about 6 min) shows the rapid decreases of hardness and line breadth, which indicates that the HTMT specimen undergoes static recrystallization during this period. However, as the holding time increases, the hardness and line breadth tend to increase slightly. It is concluded that the slowing down of recrystallization is due to the precipitation of carbides of alloying elements in the austenite structure. This agrees with Tushinskii *et al.* [15] and Bol'shakov *et al.* [12] who have reported that when hot-worked low-alloy steel was held isothermally after hot-working for about 7 min the precipitation of alloy carbides was observed in the hot-deformed austenite structure, which retarded the process of recrystallization in the austenite grains. This recrystallization process agrees with the microstructural observations of austenite grains in Fig. 9. Fine equi-axed recrystallized grains are observed after isothermal holding for 6 min, which corre-

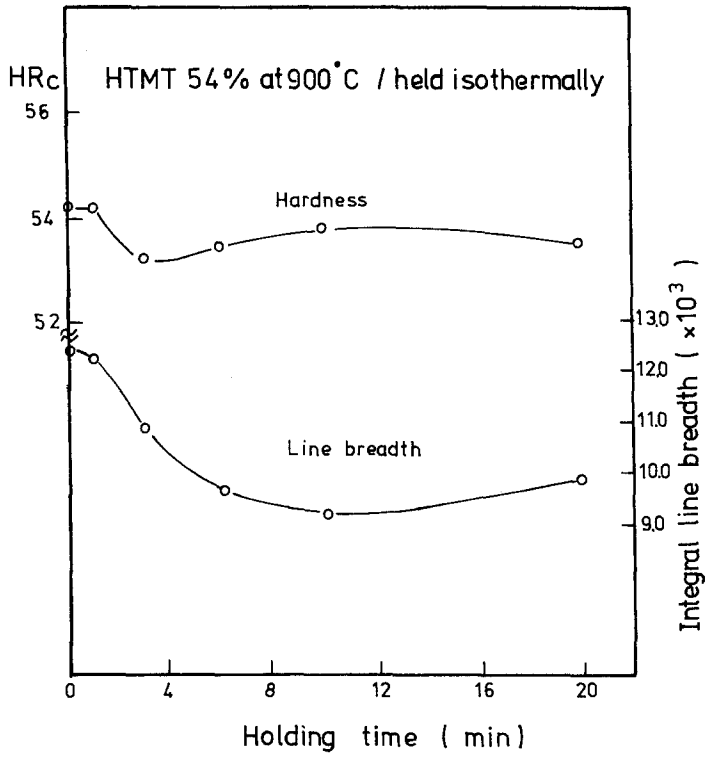

Figure 8 Changes of hardness and $(1\,1\,0)_M$ integral line-breadth as a function of holding time after hot deformation at 900° C.

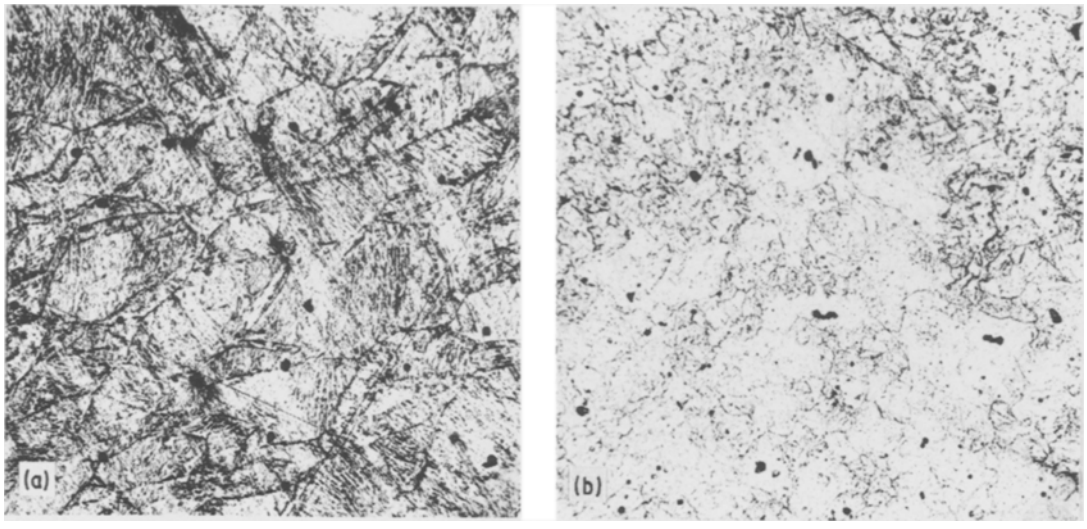

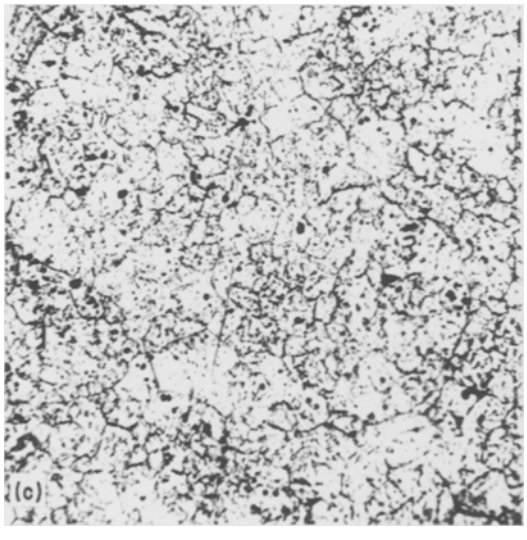

Figure 9 Recrystallization of the austenite grain of HTMT 54% specimen with holding time at 900° C (× 390). (a) 1 min, (b) 6 min, (c) 20 min.

sponds to the result shown in Fig. 8 (Fig. 9b). Further isothermal holding for 20 min results in the growth of the recrystallized grains shown in Fig 9c. Consequently, considering the results of line broadening, hardness, and microstructural observation, it can be concluded that in this study dynamic recovery and recrystallization during HTMT was a minor factor, so there was no unfavourable effect of HTMT on the precipitation of carbide.

3.4. Mechanical properties

Fig. 10 shows the effect of HTMT on tensile properties and hardness. All the specimens were tempered at 600° C for 1 h. It was found that ultimate tensile strength (UTS), and yield strength similarly increase with increasing degree of deformation. In the case of yield strength, the highest value of 135 kg mm^{-2} was obtained for the HTMT 54% specimen, on the other hand, the lowest yield strength of 107 kg mm^{-2} was for the CT specimen. It follows from this result that HTMT increases the strength of steel as compared to CT (conventional treatment). From the microstructural observation, it is believed that the increase in strength is due to refinement of the martensite structure and distribution of fine carbide precipitates within the martensite lath. In particular, this is believed to be a reasonable conclusion in accordance with the report [20] that the strength of tempered martensite increases primarily due to refinement of martensite structure and carbide precipitates.

Fig. 11 shows the impact energy plots for the HTMT and CT specimens over the range −196 to 100° C. All the specimens were tempered at 600° C for 1 h. As a measure of toughness in steel, the ductile–brittle transition temperature was determined from the above curves, where the ductile–brittle transition temperature was the temperature which corresponds to the medium value between minimum and maximum impact energy of each specimen over all the test temperatures. As shown in Fig. 12, the ductile–brittle transition temperature decreases steeply with increasing degree of deformation, which means that the toughness of steel is appreciably improved by the HTMT process. Additionally, the fracture surface of the specimen tested at −40° C was

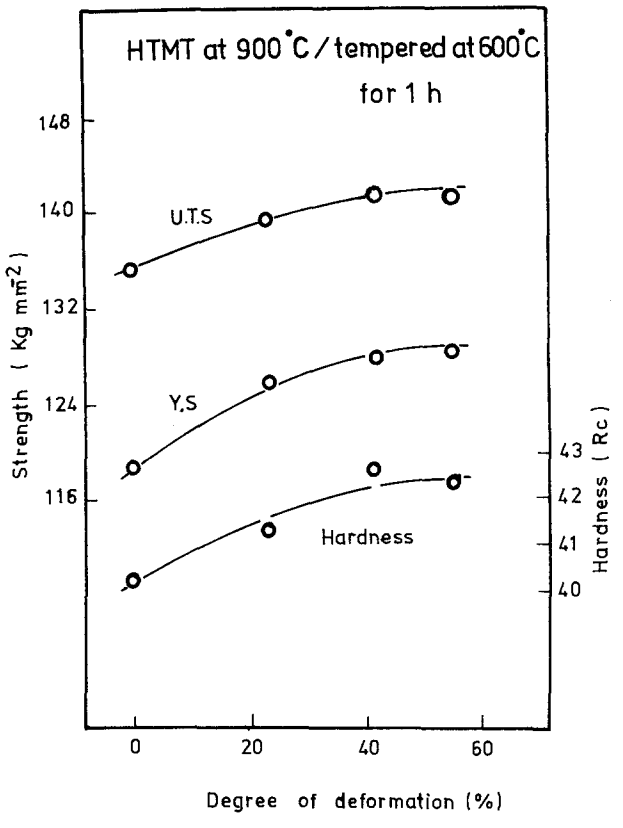

Figure 10 Effect of HTMT on tensile properties and hardness as a function of degree of deformation.

observed by scanning electron microscopy (Fig. 13). The CT specimen (Fig. 13a) shows a fracture mode of interlath cleavage while the HTMT specimen (Fig. 13b) shows a more ductile fracture mode having dimple structure. It can be concluded that HTMT considerably improves the toughness of steel as compared to CT (conventional treatment). Needless to say, this results from the refinement of martensite structure and the random distribution of fine carbide precipitates. This can be explained as follows. In the CT specimens, the rod-like coarse cementite is mainly precipitated in the region of the grain boundary, which hinders the movement of dislocation and generates subsequent stress concentrations around the precipitates, resulting in a brittle fracture mode [21, 22].

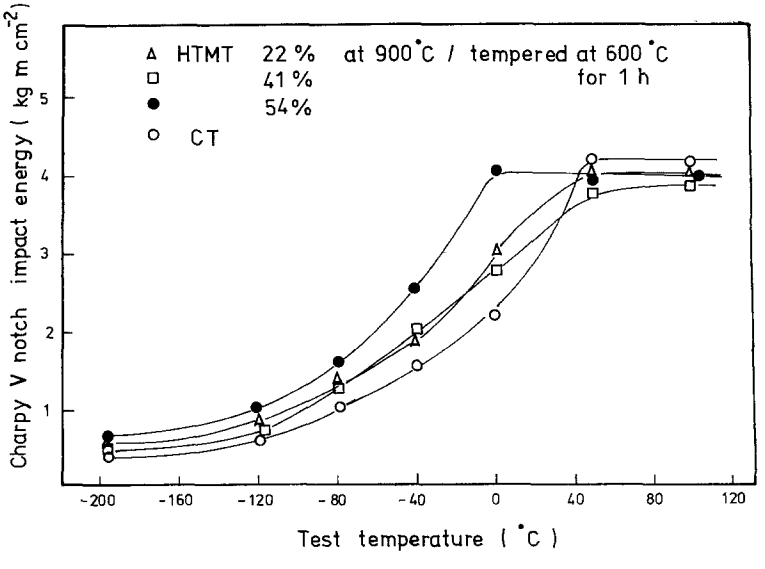

Figure 11 Effect of HTMT on ductile–brittle transition temperature as a function of degree of deformation.

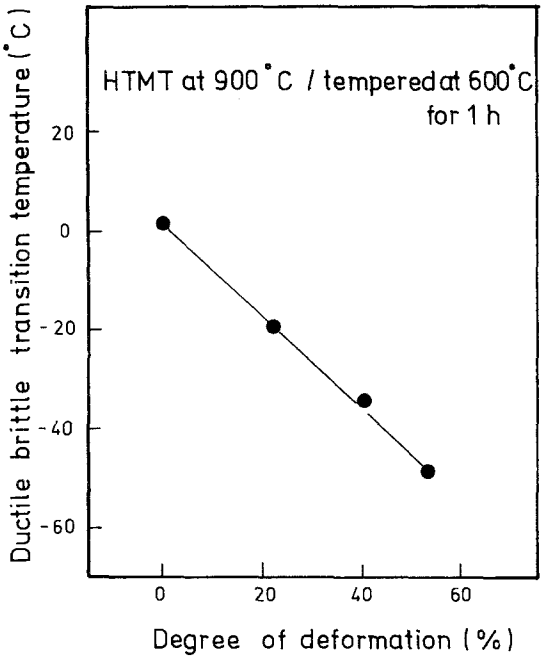

Figure 12 Effect of degree of deformation on ductile–brittle transition temperature.

This is consistent with the observations in Fig, 13 [23]. On the other hand, the random distribution of fine carbide of HTMT largely reduces the brittle fracture. Consequently, the fracture surface for the HTMT specimen reveals a more ductile fracture mode having a dimple structure as shown in Fig. 13b.

4. Conclusions

(1) HTMT improves the mechanical properties, especially the toughness, of steel compared to CT (conventional heat treatment). The strength and toughness increase with increasing degree of deformation by HTMT, particularly since ductile–brittle transition temperature as a measure of toughness decreases steeply with increasing degree of deformation. In view of this, the CT specimen shows the brittle fracture mode of interlath cleavage while the HTMT specimen reveals the ductile fracture mode having a dimple structure.

(2) The kinetics of carbide precipitation during tempering are enhanced by the HTMT process. The change of hardness with tempering time at 600° C shows that tempering resistance corresponding to secondary hardening due to fine alloy carbide occurs faster as the degree of deformation increases.

(3) From the analysis of line broadening on $(1\,1\,0)_M$ and hardness change with holding time after hot-deformation, the dynamic recovery and recrystallization during HTMT are believed to be inhibited. Owing to this, the random distribution of fine carbide in martensite structure is hardly affected, and from observation of the microstructure, HTMT also refines the martensite structure.

(4) Considering points 1 to 3, the improvement of mechanical properties by HTMT is due to the distribution of fine carbide precipitates within the martensite lath and the refinement of martensite structure.

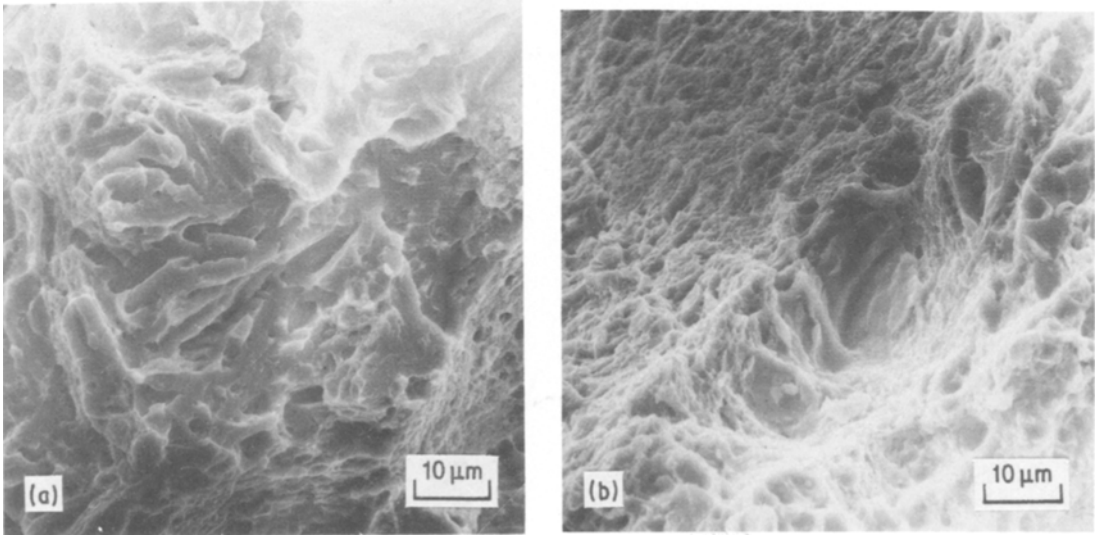

Figure 13 Fracture surfaces of tempered martensite specimens impact tested at – 40° C. (a) CT, (b) HTMT 54%.

References

1. M. Kh. SHORSHOROV, *Metal Sci. J.* 7 (1973) 213.
2. E. M. H. LIPS and H. VAN ZUILEN, *Met. Prog.* 66 (1945) 103.
3. ERIC B. KULA and S. VICTOR RADCLIFFE, *J. Metals* 10 (1963) 755.
4. L. HYSPECKÅ, *Sbornfk věd Prac. VŠB*, 16 (1970) 1.
5. L. HYSPECKÅ and K. MAZANEC, *Mém. Sci. Rev. Méetall.* 68 (1971) 305
6. *Idem, J. Iron Steel Inst.* 205 (1967) 1261.
7. R. ROUSSEV, *Mem. Sci. Rev. Met.* 67 (1970) 173.
8. J. ROFES-VERNIS, *Met. Corr, Ind.* 46 (1973) 173.
9. MAMORU NAKAMURA, HITOSHI ASAMURA and KYUHIKO YAMANANKA, *Nippon Gakkaisi* 32 (1968) 1043.
10. *Idem, ibid,* 32 (1968) 1052.
11. M. TVRD'Y, L. HYSPECKÅ, and K. MAZANEC, *Met. Tech.* 3 (1978) 73.
12. V. I. BOL'SHAKOV, L. I. KOTOVA and I. A. MONGAIT, *Metall. Term. Obrabot. Metallov.* 2 (1976) 28.
13. G. VENKATARAMAN and A. K. MALLIK, *Trans, Iron Steel Inst. Japan* 13 (1973) 192.
14. G. VENKATARAMAN and A. K. MALLIK, *Materi. Sci. Eng.* 16 (1974) 133.
15. L. I. TUSHINSKII, L. B. TIKHOMIROVA and P. V. RESHED'KO, *Metall. Term. Obrabot. Metallov.* 2 (1974) 15.
16. G. R. SPEICH, *Trans. AIME.* 245 (1969) 2553.
17. G. R. SPEICH and W. C. LESLIE, *Met. Trans.* 3 (1972) 1043.
18. EDGAR C. BAIN and HAROLD W. PAXTON, "Alloying Ellements in Steels", (ASM, Metals Park, Ohio, 1966) p. 218.
19. B. D. CULLITY, "Elements of X-ray Diffraction" (Addison-Wesley, New York, 1967) p. 262.
20. D. W. SMITH and R. F. HEHEMANN, *J. Iron Steel Inst.* 209 (1971) 476.
21. A. H. COTTRELL, *Trans. AIME.* 4 (1958) 192.
22. R. E. DOLBY and J. F. KNOTT, *J. Iron Steel Inst.* 10 (1972) 657.
23. R. M. HORN and ROBERT O. RITCHIE, *Met. Trans.* 9A (1978) 1039.

Received 5 June and accepted 6 November 1980.